Published online 4 October 2015

Nucleic Acids Research, 2016, Vol. 44, No. 3 ***e26***
doi: 10.1093/nar/gkv971

Attomole quantification and global profile of RNA modifications: Epitranscriptome of human neural stem cells

Maria Basanta-Sanchez[1,*], Sally Temple[2], Suraiya A. Ansari[2], Anna D'Amico[1] and Paul F. Agris[1]

[1]The RNA Institute, University at Albany, Albany, NY, USA and [2]Neural Stem Cell Institute, Rensselaer, NY, USA

Received July 10, 2015; Revised August 21, 2015; Accepted September 15, 2015

ABSTRACT

Exploration of the epitranscriptome requires the development of highly sensitive and accurate technologies in order to elucidate the contributions of the more than 100 RNA modifications to cell processes. A highly sensitive and accurate ultra-high performance liquid chromatography—tandem mass spectrometry method was developed to simultaneously detect and quantify 28 modified and four major nucleosides in less than 20 min. Absolute concentrations were calculated using extinction coefficients of each of the RNA modifications studied. A comprehensive RNA modifications database of UV profiles and extinction coefficient is reported within a 2.3–5.2 % relative standard deviation. Excellent linearity was observed 0.99227–0.99999 and limit of detection values ranged from 63.75 attomoles to 1.21 femtomoles. The analytical performance was evaluated by analyzing RNA modifications from 100 ng of RNA from human pluripotent stem cell-derived neural cells. Modifications were detected at concentrations four orders of magnitude lower than the corresponding parental nucleosides, and as low as 23.01 femtograms, 64.09 attomoles. Direct and global quantitative analysis of RNA modifications are among the advantages of this new approach.

INTRODUCTION

The study of RNA modifications—'epitranscriptomics'—is recognized as a new frontier for identifying their biological importance as a code to RNA's control to gene expression, and as possible diagnostic biomarkers with a great potential for therapeutic invention (1–5). The distinctive chemistries of the over 100 post-transcriptional, enzymatic modifications of RNA are critical to RNA structure, its conformation dynamics and function (2,6–8). Modifications of the epitranscriptome change in response to internal signals or external insults, impacting fundamental aspects of cell and molecular behavior (4,9,10) yet the mechanisms and processes involved are largely unknown. The recording of temporal changes in these many RNA modifications in association with development, disease, drug or environmental exposure is a challenge but will provide insight into our understanding of their impact on RNA regulation of cellular function.

Significant challenges hinder our comprehension of the role of RNA modifications in gene regulation. The most interesting of modified nucleoside functions reside in the least abundant of RNAs particularly non-coding RNA and mRNAs of eukaryotes at the femtogram and attomole levels (11–13). Modified nucleosides change with time, an RNA may not be modified 100%, and the more complex modifications requiring multiple enzymes may be incompletely modified. While the least abundant of RNAs can be amplified, present technologies for the most part exclude modifications. The exceptions are a small number of RNA modifications, pseudouridine (Ψ), inosine (I), 6-methyladenosine, (m^6A), 6-methyl-2′-Omethyladenosine (m^6Am) and 5-methylcytidine, (m^5C) (14–16). Therefore, advancement in modified nucleoside analysis needs to address the identification of a large number and chemically diverse modifications simultaneously and accurately with reproducible quantitation at the attomole level, with speed, high-throughput, ease and widely applicable workflow and versatility to assess changes in modification with time.

Ultra-high performance liquid chromatography (UHPLC) coupled with tandem mass spectrometry (MS/MS) provides a high level of accuracy, sensitivity and selectivity (17). Complete enzymatic digestion of the RNA to its constituent nucleosides under physiological conditions preserves the most complex of modification chemistries because many are susceptible to alkaline, acidic, free radical and oxidative conditions (18,19). In the absence of the phosphate, liquid chromatography separation of the mononucleosides is predominated by the modifications yielding re-

*To whom correspondence should be addressed. Tel: +1 518 591 8815; Fax: +1 518 437 4456; Email: mbasantasanchez@albany.edu

producible base line separations in minutes (18). Technology developments have resulted in higher sensitivities and lower limits of detection, thereby permitting direct analysis avoiding amplification (5,10,17,20,21). These recent improvements together with exciting discoveries of the regulatory function of RNA modifications (15,22–24), provide the motivation to push the technology even further. The goal is easily adopted techniques and methods allowing attomole sensitivities and simultaneous accurate and direct quantification of many of the RNA modifications in all biological systems, across RNA types and abundances.

Accurate quantitation of each nucleoside is essential for understanding the biology of the epitranscriptome and its possible biomedical implications and applications. However, the accuracy of the measurements is dependent on the accuracy of each nucleoside's extinction coefficient derived from measurements of UV absorbance. Extinction coefficients of major RNA nucleosides are readily available with coefficients variance of 2.0–10.0% (25). However, this is not true for the modified nucleosides, making quantitative measurements of modification a challenge. Here, we report spectrometric techniques for the calculation of extension coefficients for 28 different RNA modifications. The newly determined extinction coefficients were then incorporated into the development of a highly sensitive and accurate UHPLC–MS/MS method with an average limit of detection (LOD) at the attomole, femtogram level, demonstrating sensitives greater than previously reported (9,26–28). The applicability of the method was evaluated by investigating the presence of RNA modifications with as little as 100 ng of total RNA from human pluripotent stem cell-derived, neural stem cells. A wide variety of RNA modifications were detected at levels as low as 0.0023 pg/μl, 64.09 attomoles. These results illustrate the potential capabilities and applicability of the methods and technologies developed to provide unique insights into the mechanisms of development and disease that may lead to novel diagnostics and therapeutics.

MATERIALS AND METHODS

Materials

All of the purchased nucleosides and modified nucleosides were of highest commercial purity (Supplementary Table S1). We received a gift of a small number of nucleosides from Dr Andrzej Malkiewicz (Technical University, Lodz, Poland) and from Alexander Deiters (University of Pittsburgh, Pittsburgh, PA, USA) that underwent lyophilization and were stored at −20 °C. Isotopically labelled guanosine was a gift from Cambridge Isotope Laboratories, Inc.. A commercially available nucleoside text mixture was used for day to day instrument evaluation (Sigma–Aldrich Co.). All of the nucleoside standards were characterized individually by direct infusion MS. If degradation or impurities were present, these preparations were discarded from further analysis. Signs of oxidative degradation were not observed. This was avoided by using 18 mΩ water obtained through filtration and not by distillation, by performing enzymatic rather than chemical digestion, and by performing the analysis of nucleoside composition directly after digestion of the RNA. Even some of the most susceptible of modifications to oxidation, the thiolated nucleosides, were found to be stable.

Reagents for the enzymatic digestion of RNA included: ammonium acetate, ammonium bicarbonate, nucleoase P1 from *Penicillium citrinum (*# N8630) and phosphatase alkaline from *E.coli* (#P5931). Acetonitrile (LC–MS Optima) was purchased (Fisher).

Extinction coefficient determinations

Due to the dependency of the extinction coefficient on buffer conditions, individual solutions of major and modified nucleosides were prepared in 0.01 % formic acid in water at pH 3.5, suitable for UHPLC–MS/MS analysis. Each nucleoside was weighed to a final mass of 1 mg ± 0.001 on a XP26 balance (Mettler-Toledo). Nucleosides were dissolved on 0.01 % formic acid in water and measured by mass to a final volume of 19.0 ± 0.01 g. The density value used in the study was equivalent to that of water at 22 °C. Nucleoside solutions were heated to 60 °C for 20 min and cooled down to room temperature to ensure complete dissolution. Three replicates were prepared per nucleoside.

UV absorbance measurements were performed on a Cary Series UV-Vis spectrophotometer (Agilent). Instrument parameters used during UV measurements included wavelength, scanned from 340 nm to 190 nm; average time, 0.2 s; data interval, 1 nm: scan rate, 300 nm/min; and temperature, 25 °C. A reference was used at all times containing the same buffer as the nucleoside solutions to allow background subtraction. Absorbance measurements were collected in triplicates for each of the individual nucleoside replicates. Mass-based dilutions were conducted to ensure that the A_{260} reading fell between 0.5 and 1.5 being the optimum range by which the instrument will offer maxima accuracy of measurements as recommended by instrument manufacturer. The UV measurements were made on the same day as nucleoside solutions were prepared to avoid possible source of errors due to evaporation, sample degradation or bacterial growth.

The extinction coefficient was calculated following the Beer-Lambert equation: $\varepsilon = \frac{A}{c*l}$, where ϵ = extinction coefficient $lmol^{-1}cm^{-1}$, A = absorbance, c = concentration of solution in mol^{-1}, l = path length (1 cm). Each nucleoside solution was prepared in triplicate and each spectrometric analysis was performed three times with the extinction coefficient averaged and the associated error of analysis calculated as percentage coefficient of variance (Table 1, Supplementary Table S1).

UHPLC–MS/MS

A mixture of 4 major and 28 modified nucleosides was subjected to chromatography using a Waters ACQUITY I-Class UPLC™ (Waters, USA) liquid chromatographic system equipped with a binary pump and autosampler that was maintained at 4 °C. A Waters ACQUITY UPLC™ HSS T3 column (2.1 × 50 mm 1.7 μm) and a HSS T3 guard column (2.1 × 5 mm, 1.8 μm) were used for the separation. The assay was completed at a flow rate of 0.2 ml/min and column temperature of 25 °C. Mobile phases included RNase-free water (18.0 $M\Omega cm^{-1}$) containing 0.01 % formic acid (Buffer

Table 1. Physical and chemical parameters of major and modified RNA nucleosides. From left to right: molecular weight (MW); extinction coefficient at 260 nm (ϵ_{260}); relative standard deviation of ϵ measurements; tandem MS fragmentation molecular/product ion pair [MH^+]/[BH^{2+}]; retention time and index to Figure 2. Additional details are found in Supplementary Table SS1

Nucleosides	MW (g/mol)	ϵ_{260} ($lmol^{-1}$ cm^{-1})	RSD (%)	[MH^+]/[BH_2^+]	Retention Time (min)	Index Figure 2
adenosine (A)	267.24	11 637.51	2.73	268.2/136.1	9.03	21
N^6-isopentenyladenosine (i^6A)	335.36	15 209.44	2.53	336.0/204.6	15.58	32
N^6-methyladenosine (m^6A)	281.27	12 025.21	1.83	282.2/150.0	12.17	29
1-methyladenosine (m^1A)	281.3	11 652.45	1.47	282.0/150.0	3.01	5
inosine (I)	268.23	7145.35	2.50	269.1/137.1	8.21	15
1-methylinosine (m^1I)	282.30	5809.15	0.33	283.0/151.0	10.43	25
guanosine (G)	283.24	10 692.58	2.95	284.1/152.1	8.45	17
1-methylguanosine (m^1G)	297.27	12 203.88	1.32	298.2/166.1	10.86	27
N^2-methylguanosine (m^2G)	297.27	3176.83	1.35	298.2/166.1	10.44	24
7-methylguanosine (m^7G)	297.30	9056.63	1.60	298.1/124.0	5.09	12
2′-O-methylguanosine (Gm)	297.27	8992.65	1.60	298.1/152.0	10.40	23
cytidine (C)	243.22	6242.12	1.33	244.2/112.1	1.65	1
5-methylcytidine (m^5C)	285.25	3556.19	0.87	258.0/126.0	3.14	7
2′-O-methylcytidine (Cm)	257.20	6079.69	1.50	258.1/112.1	5.64	13
N^4-acetylcytidine (ac^4C)	257.25	7230.65	2.61	286.2/154.1	10.98	28
2-thiocytidine (s^2C)	311.29	13 071.58	2.31	260.0/128.0	4.49	11
5-formylcytidine (f^5C)	271.23	7377.26	2.31	272.1/140.0	8.73	18
uridine (U)	245.09	8912.32	1.5	245.1/113.1	4.37	10
2′-O-methyluridine (Um)	258.20	8234.70	1.09	259.1/147.0	9.52	22
5-methyluridine (m^5U)	258.23	7743.31	2.09	259.1/127.0	8.39	16
6-methyluridine (m^6U)	258.23	9651.15	1.93	259.1/127.0	6.40	14
2-thiouridine (s^2U)	260.20	8583.71	4.01	261.1/129.0	2.99	6
4-thiouridine (s^4U)	260.27	2709.52	2.36	261.3/129.01	8.96	20
5-methoxyuridine (mo^5U)	274.23	4535.23	2.01	275.2/143.1	8.81	19
5-methoxy-2-thiouridine (mo^5s^2U)	290.30	5589.84	0.89	291.1/159.0	12.30	30
5-methoxycarbonylmethyl- uridine (mcm^5U)	316.15	9182.25	1.59	317.1/185.1	10.65	26
5-methylaminomethyl-2-thiouridine (mnm^5s^2U)	303.34	7594.77	0.58	304.1/172.1	3.53	8
5-methoxycarbonylmethyl-2-thiouridine (mcm^5s^2U)	332.33	9057.22	5.28	333.0/201.0	13.44	31
5-carboxymethylaminomethyl-uridine ($cmnm^5U$)	331.28	6732.67	1.34	332.4/239.2	2.41	4
pseudouridine (Ψ)	244.20	7492.67	2.75	245.1/209.0	1.96	3
1-methyl-3-(3-amino- 3-carboxy-propyl) pseudouridine ($m^1acp^3\Psi$)	359.34	5651.09	2.29	360.1/270.1	3.99	9
dihydrouridine (D)	246.20	3500.25	2.26	246.2/113.1	1.80	2

A) and 50 % acetonitrile in aqueous 0.01 % formic acid pH 3.5 (Buffer B) (20). A 20 min gradient was developed to obtain optimum separation of modified nucleosides (Supplementary Table S2).

Tandem MS analysis of RNA nucleosides was performed on a Waters XEVO TQ-S^{TM} (Waters, USA) triple quadrupole mass spectrometer equipped with an electrospray ionization (ESI) source maintained at 150 °C and the capillary voltage was set at 1 kV. The desolvation gas, nitrogen was maintained at 500 l/h and desolvation temperature at 500 °C. The cone gas flow was set to 150 l/h and nebulizer pressure to 7 bars. Quantitative determination was performed in ESI positive-ion mode using multiple-reaction monitoring (MRM). The ion transitions, cone voltage and collision energy used for UHPLC–MS/MS were determined using MassLynx V4.1Intellistart software. Retention times and the corresponding protonated molecular and product ion pairs [MH^+/BH^{2+}] were obtained for each individual nucleoside.

Day to day reproducibility was assessed by monitoring retention time and peak area of a commercially available nucleoside mixture containing 11 nucleosides (3 major and 8 modified nucleosides) at concentrations ranging from 10 to 100 pg/μl. Each sample was injected in 3–5 replicates per day and 2.0 μl volumes. Day to day variability is expressed as percentage coefficient of variation (% CV).

Quantification of each of the 32 individual nucleoside standards included six calibration points with concentrations ranging between 0.05 and 2.0 pg/μl. All calibrations were produced in the presence of 1.0 pg/μl of isotopically labeled [^{13}C][^{15}N]-G as an internal standard (IS). Five non-consecutive replicates were run for each of the calibration points and a blank sample. The blank sample was RNAse-free water in 0.01 % formic acid solution, run between each of the replicates. A linear regression curve was produced from the data for each nucleoside standard from which the LOD and the limits of quantification (LOQ) were calculated. LOD is defined as $3\sigma/S$, and LOQ is defined as $10\sigma/S$ where σ is the standard deviation of the intercept and S the slope of the calibration curve (29).

Data acquisition and analysis were performed with Masslynkx V4.1 and TargetLynx software. Calibration curves for the 32 standards were generated using an internal standard ratio determined in OriginPro 2015. Concentrations of the nucleosides originating from neural stem cell RNAs were calculated using the internal standard added to the RNA prior to its hydrolysis. A ratio of each nucleoside signal from the RNA sample to that of the internal standard was compared to the same ratio calculated from the standard nucleoside calibration curve. The final concentration is expressed as the mean and standard deviation of five non-consecutive technical replicates for each biological replicate. To evaluate the performance of the method, we compared RNA samples obtained from five stages of differentiation of the pluripotent to neural cells.

H9 human cells culture

Human ES cells (H9, WiCell) were cultured on irradiated mouse embryonic fibroblasts (MEFs) (GlobalStem) in HES-medium (Life Technologies): DMEM/F12 (1:1) with 20% (v/v) KSR, 100 μM non-essential amino acids, 1 mM L-glutamine, 55 μM 2-mercaptoethanol and 10 ng ml-1

FGF2 (30). Human ES cells were dissociated to single cells using dispase (StemCell). ES cells (10^5) were plated into each well of a 24-well plate previously coated with matrigel (BD biosciences). Cells were grown in HES-medium conditioned on MEFs. ROCK inhibitor was added to the medium prior to use (Stemgent). When HES cultures were approximately 90 % confluent, induction of neural progenitors was initiated using an adaptation of a rapid (12 days) dual SMAD inhibition protocol (31,32). The medium was changed daily for the first three days. The culture medium used on the first and second days was KSR medium. All reagents for knockout serum replacement (KSR) medium were obtained from a single supplier (Life Technologies) unless indicated otherwise: knockout-DMEM with 15 % (v/v) KSR, 2 mM L-glutamine, 100 μM non-essential amino acids, 55 μM 2-mercaptoethanol, supplemented with 100 nM LDN193189 (Stemgent) and 10 μM SB431542 (Tocris). On the third day, 1 μM cyclopamine (Stemgent) was added to the KSR medium. After the third day, the medium was changed every other day. The culture medium was changed from KSR medium to N2-medium gradually. From day five, increasing amounts of N2-medium were added with each feeding (25, 50, 75 and 100 %). During this period, the cyclopamine concentration was maintained at 1 μM. N2-medium consisted of: DMEM/F12 (1:1) (Life Technologies) with N-2 supplement and 0.775 g glucose (Sigma). On day 13 after starting neural induction, the medium was changed to a culture medium supporting cortical differentiation and adapted from the published composition (33), changed every other day. This medium designated N2/B27 consisted of equal parts (1:1) 'adapted N2-medium' and 'B27 medium'. Adapted N2-medium and B27 medium reagents were obtained from Life Technologies. Adapted N2-medium was composed of DMEM/F12 (1:1) with N-2 supplement plus 2 mM L-glutamine, 0.5 mg/ml[1] bovine albumin fraction V solution, 110 μM 2-mercaptoethanol and 10 ng/ml FGF-2. B27 medium was comprised of Neurobasal with B-27 supplement, 2 mM L-glutamine, supplemented with 10 ng/ml FGF-2 added freshly before feeding to promote cortical progenitor proliferation and neurogenesis (34).

Isolation and purification of RNA

Cells were harvested by centrifugation, the supernatant removed and total RNA extracted from cells using the RNeasy plus mini kit (Qiagen) according to the manufacturer's specifications. RNA was extracted from one biological replicate at various stages of stem cell differentiation on: Days 0, 7, 19, 49 and 77 (31). RNA samples were treated with RNAse-free, DNAse I (LifeTechnologies) followed by ethanol precipitation. RNA recovery was 11.21 ± 3.12 μg. The average 260/280 nm ratio of 2.01 ± 0.03 represented a high degree of purity and reproducibility of the extraction protocol. RNA pellets were lyophilized and stored at −80 °C until the final 77-day sample was obtained before proceeding with UHPLC–MS/MS analysis.

Enzymatic hydrolysis of RNA

Whole cell RNA, 100 ng, was hydrolyzed to the composite mononucleosides via a two-step enzymatic hydrolysis (18,19,35). The first step of phosphodiester bond cleavage was accomplished with nuclease P1 resulting in nucleoside-5′-monophosphates. Optimum nuclease P1 activity was achieved at pH 5.5 by addition of 1/10 volume of 1.0 M ammonium acetate pH 5.5 and the pH change confirmed. For each 0.5 absorbance unit of RNA, 2 units of nuclease P1 were added and incubated overnight at 37°C. The second step of nucleoside preparation uses bacterial alkaline phosphatase (BAP) to cleave the 5′-phosphate from the nucleosides resulting in individual nucleosides and phosphoric acid. For optimum BAP activity, the pH was adjusted to pH 8.3 by adding a 1/10 volume of 1.0 M ammonium bicarbonate pH 8.3. One unit of BAP was added for each 0.5 absorbance units of RNA and incubated at 37 °C for 2 h. The nucleoside products were lyophilized and stored at −20 °C. Samples were reconstituted in RNAse-free water prior to UHPLC–MS/MS analysis.

RESULTS

Extinction coefficient and UV profiles of modified nucleosides

To calculate absolute concentrations of RNA modifications, we determined their extinction coefficients under buffer conditions that matched those used for mass spectrometry at pH 3.5. UV spectra were recorded for each of the 4 major and 28 modified nucleosides (Figure 1) prepared in triplicate and each analyzed on the spectrophotometer 3 times. Each of the modifications exhibited a spectrum that greatly differed from that of the parental unmodified nucleoside as can be seen for the s^4U and dihydrouridine, D, spectra (Figure 1) with a λmax around 330 nm and 210 nm regions, respectively, as compared to that of U with λmax 260 nm. The extinction coefficients of all of the nucleosides were calculated at 260 nm, as well as that at the absorbance maximum nearest 260 nm (Table 1, Supplementary Table S1). Average error for ϵ_{260} and ϵ_{max} was expressed as the percentage of the relative standard deviation (%RSD) and ranged from 0.2 to 4.0 %. Spectrometric deviations resulted in less than 0.5 % error compared with weight measurements that result in a 1.0–4.0 % error (data not shown). Previous studies have reported quantities of modified nucleosides by calculating relative peak areas to that of their parental nucleosides, A, G, C and U (22,36). However, should the final goal of the study be absolute quantitation of modified nucleosides, the ratio between the extinction coefficients of the modified nucleoside and that of the parental nucleoside needs to be carefully considered (Supplementary Table S1). The error in these relative measurements is appreciated by examining the ratio of extinction coefficients of the modified nucleoside and its parental nucleoside. Based on these ratios, errors in calculating concentrations ranged from 0.1 % as in the case of 1-methyladenosine to adenosine (ϵ_{260} m^1A/ϵ_{260} A = 1.001), to as high as 69.6 % as in the case of 4-thiouridine/uridine (ϵ_{260} $s^4U/\epsilon_{260}U$ = 0.3004). This characteristic distinction is also realized by comparing the UV spectra (Figure 1). Extinction coefficients for A, G, U and C have been reported at pH ∼6.8 (25). For the purpose of this study, extinction coefficients were calculated at buffer conditions optimal for nucleoside mass spectrometry at pH 3.5. However, to test the reliability of the protocol, extinction coefficients for A, G, U and C were calcu-

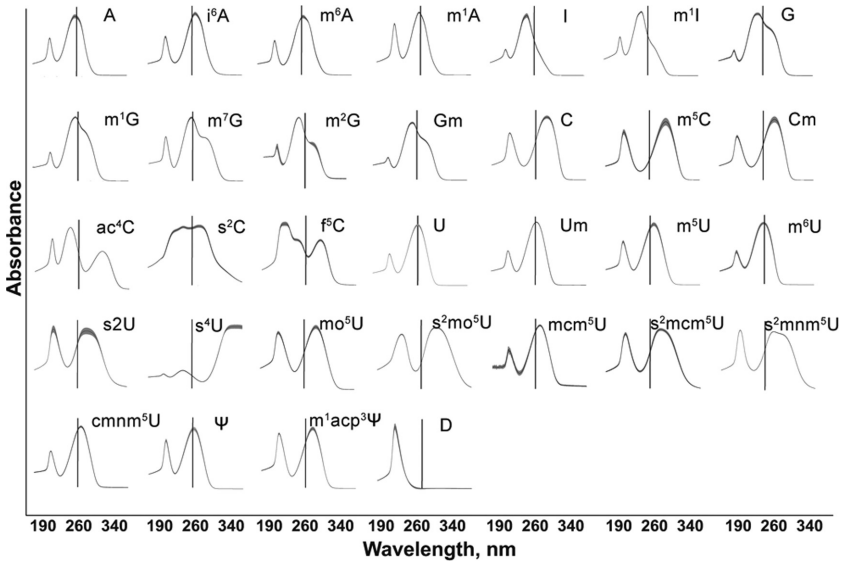

Figure 1. Averaged UV-spectra of major and modified nucleosides. X-axis is represented by the wavelength range from 190 to 340 nm. The Y-axis is in absorbance units. The absorbance at 260 nm is indicated by a vertical line. Nucleoside concentrations were calculated by measuring absorbance at 260 nm and using extinction coefficients calculated at pH 3.5 (Table 1). Standard deviation from multiple scans and experiments is represented by the gray shadow (Further details can be found in the Supplementary Information).

lated following the same protocol described here, but with a phosphate buffer solution at pH 6.8. Resultant ϵ_{260} values were compared to previously reported values (25) with agreement between 0.71 and 3.4 % (Supplementary Table S3). An exception was the highest calculated error of 5.2 % RSD for adenosine. The source of this error is attributed to adenosine's hydrophobicity and its experimental concentration being close to the limits of its solubility (37).

UHPLC–MS/MS method development

Instrument reproducibility is a variable to consider in assessing the robustness of the system and capabilities of the method to examine biological samples. Day to day reproducibility was monitored by extracting retention time and peak area of a commercial nucleoside test mixture (Supplementary Figure S1). In agreement with findings reported previously (11), A, m^6A and 3-methyluridine (m^3U) were detected in addition to the nucleosides the company had included in the mixture. Based on the levels present, m^6A was probably a product of m^1A isomerization, increasing in concentration over time. A and m^3U, present in small concentrations and at constant levels, were probably impurities carried over from the synthesis of m^1A and m^5U, respectively. The retention times were highly reproducible with a percent coefficient of variation ranging between 0.62–1.32 (%CV) that matches the precision previously reported (Supplementary Table S4) (11). Reproducibility of the majority of the nucleosides peak areas was good with values ≤10% CV. However, 7-methylguanosine (m^7G) and adenosine exhibited 16.19 % and 20.45 % CV, respectively. Adenosine was found in this commercial standard mixture as a contaminant at low levels and produced higher day to day variation. The peak area for m^7G decreased over time suggesting degradation (Supplementary Figure S1, right panel).

The four major and 28 modified nucleosides were separated by UHPLC in less than 20 min and detected by MS/MS (Figure 2A). The 20 min separation represents half the ∼40 min previously reported (9,17,20). The average full width half maxima peak width obtained for the nucleosides under study was 5.7 ± 1.32 s, allowing fast and high resolution. The nature of the modification is confirmed through tandem MS. Tandem MS provides a second dimension analysis whereby the induction of collision energy as the ions pass through the collision cell will produce specific molecular ion pairs. Generally, the nucleoside molecular ion (MH^+) is fragmented at the glycosidic bond providing the product ion (BH^{2+}) and the neutral sugar residue (Supplementary Figure S2) (38). The resultant ion-pairs were inserted into the MS method for accurate separation and quantification of nucleosides with ESI positive-ion mode using MRM (Figure 2B and Table 1). The efficiency of this two-dimensional separation is well exemplified by close eluting peaks, such as G and 5-methyluridine (m^5U), with retention times of 8.45 min and 8.39 min and MRM 284.1→152.1 and 259.1→127.0, respectively. An additional example is observed for 5-formylcytidine (f^5C) and 5-methoxyuridine (mo^5U), eluting at 8.73 and 8.81 min and MRM of 272.1→140.0 and 275.2→143.1, respectively (Table 1).

The superiority of having two degrees of separation and analytical data provided by the synergy of retention time by UHPLC and mass by MS/MS becomes more evident during the separation of positional isomers. Four monomethylated isomers of G, 7-methylguanosine (m^7G), 2-O′-methylcytidine (Gm), 2-methylguanosine (m^2G) and 1-methylguanosine (m^1G) have the same mass, [MH^+]: 298.2 mass units. The elution times were 5.09, 10.40, 10.44 and 10.86 min, respectively. Thus, Gm and m^2G elute with significant chromatographic overlap (Figure 2A, peaks 23 and 24). However, m^2G fragments with MRM 298.2→166.1,

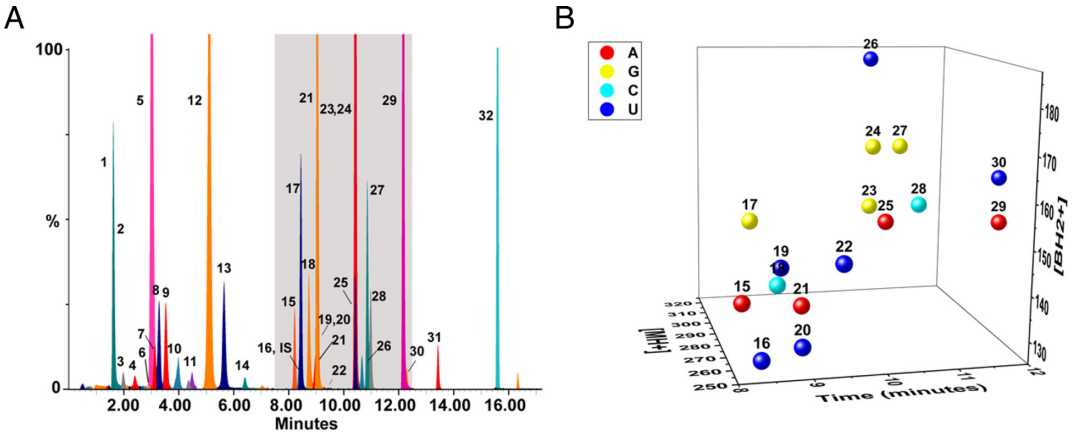

Figure 2. Extracted ion chromatogram of the four the major nucleosides, A, G, U and C and 28 modified nucleoside standards. The one-dimensional separation is shown on the left (**A**). The full names of the nucleosides are found in Table 1 with the following peak identification: 1, C; 2, D; 3, Ψ; 4, cmnm^{5}U; 5, m^{1}A; 6, s^{2}U; 7, m^{5}C; 8, mnm^{5}s^{2}U; 9, m^{1}acp^{3}Ψ; 10, U; 11, s^{2}C; 12, m^{7}G; 13, Cm; 14, m^{6}U; 15, I; 16, m^{5}U; IS, [^{13}C]$_{10}$,[^{15}N]$_5$G; 17, G; 18, f^{5}C; 19, mo^{5}U; 20, s^{4}U; 21, A; 22, Um; 23, Gm; 24, m^{2}G; 25, m^{1}I; 26, mcm^{5}U; 27, m^{1}G; 28, ac^{4}C; 29, m^{6}A; 30, mo^5 s^{2}U; 31, mcm^{5}s^{2}U; 32, i^{6}A. To ilustrate the resolution achieved for separation of the nucleosides in the time and mass dimmensions, the period of 8 to 12 min (shadowed area) is represented in a 3D plot (**B**). The time axis is the X-axis, molecular ion mass [MH$^+$] is the Y-axis and the product [BH$_2^+$] mass ions are on the Z-axis. Each of the four color representation is a canonical parental nucleoside and/or its corresponding modifications eluting during 8–12 min.

while Gm having a methylation on the 2′-O position of the ribose results in a different MRM 298.1→152.0 (Supplementary Figure S3). Thus, this method provides excellent separation and identification of modified nucleosides.

Calibration curves demonstrated the sensitive detection and accuracy in the quantitation of nucleoside modifications. Six different concentrations of each of the 4 major and 28 modified nucleosides were prepared (0.05–2.0 pg/μl) and 5 non-consecutive replicates were subject to analysis. All calibrations contained 1.0 pg/μl of isotopically labeled [^{13}C][^{15}N]-guanosine (Cambridge Isotope Laboratories, Inc.) as an IS. The intercept and the standard error, σ, represented by the standard deviation were calculated (Supplementary Table S5) for each calibration curve (Supplementary Figure S4). Curves resulted in excellent linearity (R^2 of 0.99227–0.99999) representing robustness and accuracy of the method as well as the instrumentation. LOD values ranged from 0.00164 to 0.03781 pg/μl, i.e. 63.75 attomol to 1.214 femtomole, and LOQ values (limit of quantitation) ranged from 0.00547 to 0.12603 pg/μl or 0.2126 to 4.0486 femtomole (Supplementary Table S5). To our knowledge this is the first time that LOD and LOQ have been reported for such an extended number of modified nucleosides.

Post-transcriptional modification analysis of human neural stem cell RNA by UHPLC–MS/MS

Recent technology advances have revealed exciting discoveries regarding the relevance and functions that individual RNA modifications, such as m^{6}A, I or m^{5}C have on biological processes and as signatures for changes in the epitranscriptome (22,39–41). However, most of these studies are focused on a single modification and detection levels were in the microgram to picogram range (20). To assess the potential and validity of the UHPLC–MS/MS methods as a single-step analysis of a significant number of modifications at the picogram to femtogram levels, we analyzed the epitranscriptome of human pluripotent stem cells undergoing differentiation. Changes in the epitranscriptome whether programmed or the result of external cues can impact well-established neurological pathways (42–44). Recent studies have revealed roles for m^{6}A in mRNAs, in cellular signaling, stem cell development and neurodegeneration processes (2,3,14,21,23). A comprehensive survey of RNA modifications in the human brain has not yet been described, due to the limitations in the number of RNA modifications detectable using next generation sequencing and the lack of sensitivity and standardization from direct analysis (16). Stem cells were induced to differentiate into neural cells of the prefrontal cortex (31). RNA was extracted at different times from 0.5 to 1 × 10^6 cells during the differentiation protocol, isolated and purified (Figure 3). The size distribution was evaluated by analyzing the samples (Agilent BioAnalyzer). The RNA size distribution ranged from 30 to 5000 nucleotides, with higher abundances shown in the <200 nt region, 2000 nt and 4000 nt size ranges, representative small RNAs, tRNA, rRNA and mRNAs as expected (Supplementary Figure S5). Prior to UHPLC–MS/MS analysis, 1.0 pg/μl [^{13}C][^{15}N]-G as IS was added to 100 ng of total RNA. Then, the RNA was hydrolyzed to mononucleosides. A negative control sample was included in the data set. The control was comprised of the enzymes, IS and reagents used during the enzymatic hydrolysis. Each RNA extraction was lyophilized and reconstituted with RNAse-free water, 0.01 % formic acid to a final concentration of 1ng/μl, and analyzed by UHPLC–MS/MS for the characterization of the four major and the 28 RNA modifications. Each sample was analyzed 5 times to assess instrument reproducibility. A blank sample containing only RNAse-free water in 0.01 % formic acid solution was analyzed between each of the samples to avoid cross-contamination. From the 32 initial nucleosides included in the UHPLC–MS/MS method, A, G, U and C and 19 modified nucleosides were detected above the LOD

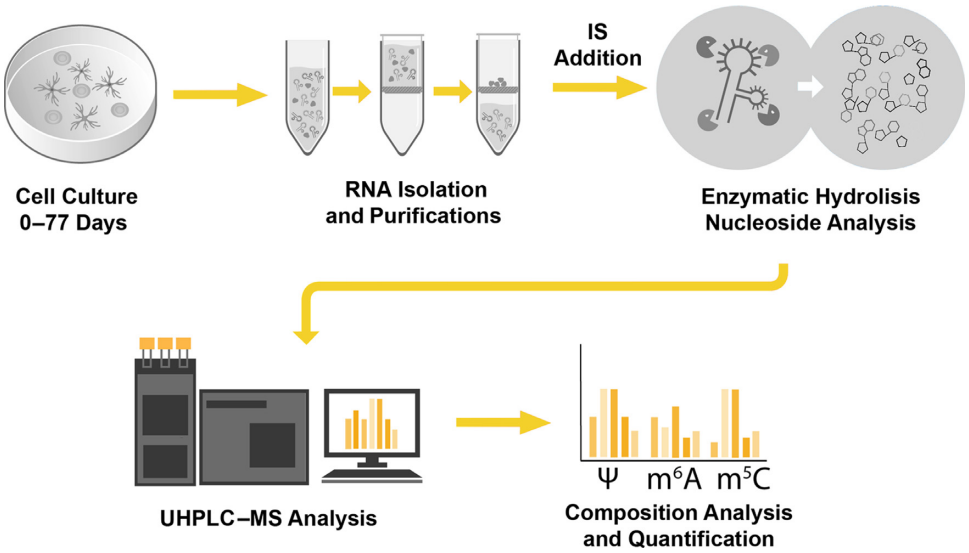

Figure 3. Experimental workflow. Graphical description of the step-by-step method for the preparation and UHPLC–MS analysis of nucleosides from total RNA extracted from cerebral cortex cells differentiated in culture. Human stem cells were cultured for 77 days and total RNA extracted, purified and readily hydrolyzed to nucleoside via a two-step enzymatic hydrolysis prior to composition analysis using UHPLC–MS/MS.

(Figure 4A–E). Those modifications below LOD were excluded from the results. The abundance and dynamic range at which RNA modifications were present varied as many as four orders of magnitude. For example on Day 0, G was the nucleoside among the 23 detected in whole cell RNA in highest concentration at 24.88 pg/μl, whereas mo^5U was present in the least amount and detected at 0.0033 pg/μl (Figure 4A, table insert). These results demonstrate the collection of both identity and quantity for a multitude of RNA modifications in a single experiment. They also show excellent instrumental capabilities to capture a broad range of concentration from picogram to femtogram, realizing an attomole level of detection of nucleoside modifications.

DISCUSSION

RNA post-transcriptional modifications are ubiquitous among the three domains of life. Many are conserved in chemistry and sequence location in specific classes of RNA, such as those of the anticodon stem and loop domain of tRNAs from all organisms (8,45). The role of RNA modifications in biological processes and relationships to human health and disease represent an untapped and importantly conserved code to RNA science and its applications (3). Advances in method and technology have enabled detection of a few RNA modifications of the epitranscriptome (1,15,22,24,36), yet with the data restricted to a few of the more than 100 RNA modifications (6,7), one has to wonder what data are missing that could aid in interpreting changes in RNA with internal signals and external cues. With accuracy and high sensitivity, the UHPLC and tandem MS method described enables identification and quantitation of 28 RNA modifications directly and simultaneously in RNAs extracted and purified from eukaryotic cells and tissues, as well as from prokaryotes. The UHPLC–MS/MS method separates minimally 28 RNA modified nucleosides and A, G, U and C, predominately at the base line and in less than 20 min. Prior LC–MS studies have shown the capacity to resolve up to 25 nucleosides in a total run time of 40–60 min (9,11,17,20). Other separations had the analysis time reduced to 15 min, but the number of nucleosides was also reduced to the canonical A, G, U and C and inosine (27). A method that incorporates a stable isotope labeled internal standard for bacterial RNA maintained a low relative standard deviation in detection of 10 modified nucleosides furthermore highlighting the importance of absolute quantification in addition to their bacterial internal standard-based quantification (28). The UHPLC–MS/MS method we have developed has the advantage of reducing the analysis time to 20 min increasing the number of nucleosides analyzed to 32 at attomole levels, and increasing the dynamic range by four orders of magnitude to accurately observe changes in the least abundant of RNA modifications.

To evaluate the utility of UHPLC–MS/MS for nucleoside composition analysis, we applied the method to one of the important, driving biological challenges, the identification and quantitation of modified nucleosides during neural stem cell differentiation. The neural stem cell model was chosen following recent studies that have revealed the importance of modifications such as m^6A, m^5C, Ψ and I, to neural signaling pathways that regulate brain development as well as stem cell biology, differentiation and cancer (2,14,46–48). We detected and identified simultaneously 21 modified nucleosides at low attomole levels in the presence of A, G, U and C and from as little as 100 ng of total RNA. The dynamic range of the method is readily observed for there is a 10^4-fold concentration difference between the major or parent nucleosides and the modified nucleosides derived from them (Figure 4). Apparent changes in the amounts of some of the modifications are observed as early as Day 19 of cell differentiation and continue through Day 77 (Supplementary Figure S6). This demonstrates proof of concept, and further replicates and analysis will enable robust conclusions to be drawn. However, we note that,

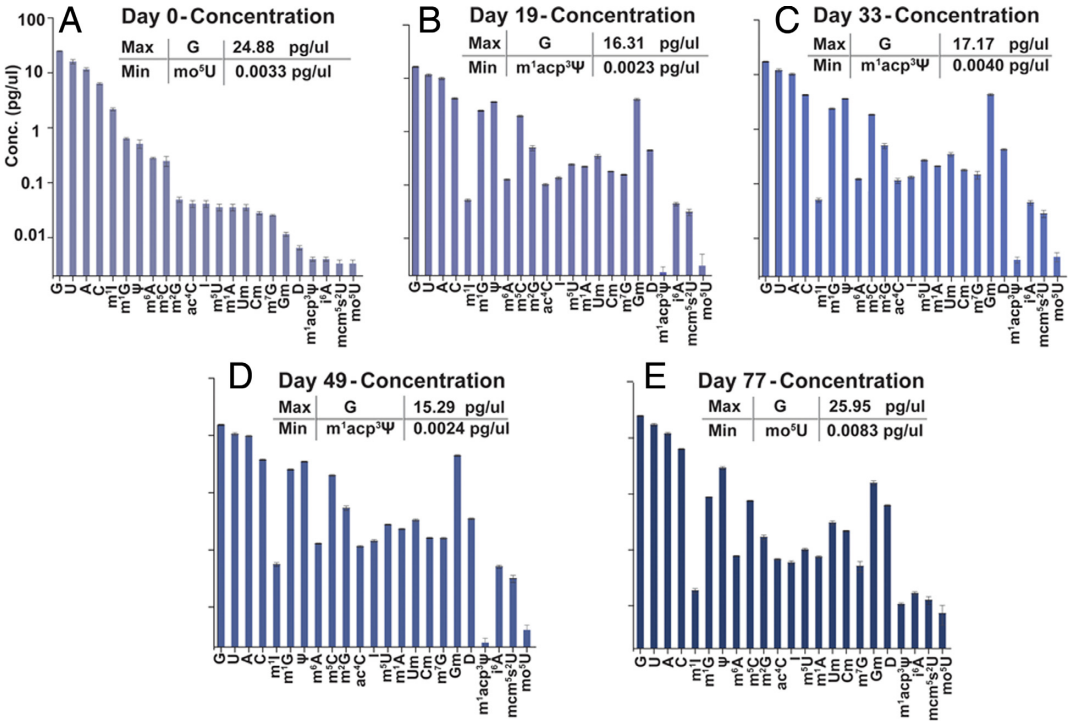

Figure 4. Absolute concentrations of RNA major and modified nucleosides during neural stem cell differentiation in culture. Day 0 (**A**), 19 (**B**), 33 (**C**), 49 (**D**) and 77 (**E**). The order of the nucleosides at Day 0 (**A**) is represented in a descending order of concentration. The Y-axis and the order of the X-axis were maintained in plots representing Day 19–77 (**B**–**E**). Dynamic range of concentrations is shown by the absolute values represented on respective tables that are inserted. The tables show that there is a 10^4-fold concentration difference between the major and modified nucleosides. Error bars represent the standard deviation of five instrument replicates.

some of the modifications that appear to have quantitatively changed during stem cell differentiation have been reported by others to have changed in mRNAs of the neural signaling pathways (2). Notably, the modifications that may be changing are found in tRNAs and rRNAs, as well as mRNA. Besides changes in the epitranscriptome attributed to mRNA, tRNA is of special interest. tRNA species are heavily modified (3,9) and the expression of particular tRNAs responds to mRNA codon requirements. Thus, tRNA species modifications are expected to change along with changes in mRNA species and modifications. Given the sensitivity of the method, upon separating subtypes of RNA from biological samples, we will be able to discern whether modifications occur on mRNA, rRNA, tRNA or miRNA species.

In this analysis, seven modified nucleosides for which standards were developed were not observed or seen below the LOD for RNA samples extracted from these cells (Supplementary Table S5): s^4U, mnm^5s^2U, m^6U, s^2C, f^5C, s^2U, mcm^5U, $cmnm^5U$ and s^2mo^5U (data not shown). The nucleoside s^4U is not observed in mammalian cells; the others were already known to be less abundant compared to others such as 2-O′-methylations. In future studies, we plan to increase the amount of material that would enable study of these low level modifications after enriching for a particular type of RNA. The ability to detect and quantify multiple RNA modifications during human pluripotent-neural stem cell studies has the potential to reveal valuable information regarding the role of RNA modifications in nervous system development and function.

Determining the presence, identity and amount of the more than 100 RNA modifications in biological samples is a very significant challenge. A reproducible and accurate method of analysis must maintain the integrity of the modified nucleosides, some of the most complex chemistries in nature. The method must be extremely sensitive in order to detect low levels at which modifications appear in the least abundant of RNAs. Previous studies have reported calibration curves in the microgram to picogram range (19). For the first time in a single-step, simultaneous, accurate detection, identification and quantitation was achieved for 28 modified nucleosides at attomole to femtomole levels in the presence of the parental A, G, U and C that occur at four orders of magnitude higher concentrations. There is a great potential for revealing functional relationships of epitranscriptome mechanisms and dynamics by investigating temporal changes in modifications during biological processes. This potential will be advanced in the near future with a high throughput, simultaneous analysis of 50 or more modifications that is affordable and user-friendly for basic science and clinical applications. Once the presence and identification of modified nucleosides even at attomole level has been linked to an important biological function, then it is critical to determine their sequence location. Thus, the coupling of the UHPLC to a sequencing of RNA by mass spectrometry is also a future research direction.

SUPPLEMENTARY DATA

Supplementary Data are available at NAR Online.

ACKNOWLEDGEMENTS

We thank Cambridge Isotope Laboratories Inc. and Maureen Duffy for their donation of isotopically labelled nucleosides, Regenerative Research Foundation and Dr K. Halvorsen and Dr S. Ranganathan for discussions and for critical reading of the manuscript.

FUNDING

Combined Funding Application (University at Albany–RNA Institute Capital Project #X765) from the State of New York; National Institute on Drug Abuse, National Institute of Health [1R41DA038983-01 to P.F.A.] in which MB-S is the principal investigator for The RNA Institute. Funding for open access charge: Research Foundation for SUNY at The University at Albany [1R41DA038983-01].
Conflict of interest statement. None declared.

REFERENCES

1. Niu,Y., Zhao,X., Wu,Y., Li,M., Wang,X. and Yang,Y. (2013) N6-methyl-adenosine (m6A) in RNA: An Old Modification with A Novel Epigenetic Function. *Genomics Proteomics Bioinformatics*, **11**, 8–17.
2. Satterlee,J.S., Basanta-Sanchez,M., Blanco,S., Li,J.B., Meyer,K., Pollock,J., Sadru-Vakili,G. and Rybak-Wolf,A. (2014) Novel RNA Modifications in the Nervous System: Form and Function. *J. Neurosci.*, **34**, 15170–15177.
3. Agris,P.F. (2015) The importance of being modified: an unrealized code to RNA structure and function. *RNA*, **21**, 552–554.
4. Saletore,Y., Meyer,K., Korlach,J., Vilfan,I.D., Jaffrey,S. and Mason,C.E. (2012) The birth of the Epitranscriptome: deciphering the function of RNA modifications. *Genome Biol.*, **13**, 175.
5. Kellner,S., Burhenne,J. and Helm,M. (2010) Detection of RNA modifications. *RNA Biol.*, **7**, 237–247.
6. Cantara,W.A., Crain,P.F., Rozenski,J., McCloskey,J.A., Harris,K.A., Zhang,X., Vendeix,F.A.P, Fabris,D. and Agris,P.F. (2011) The RNA modification database, RNAMDB: 2011 update. *Nucleic Acids Res.*, **39**, D195–D201.
7. Machnicka,M.A., Milanowska,K., Oglou,O.O., Purta,E., Kurkowska,M., Olchowik,A., Januszewski,W., Kalinowski,S., Dunin-Horkawicz,S, Rother,K.M. *et al.* (2013) MODOMICS: a database of RNA modification pathways–2013 update. *Nucleic Acids Res.*, **41**, D262–D267.
8. Agris,P.F. (1996) The importance of being modified: roles of modified nucleosides and Mg2+ in RNA structure and function. *Prog. Nucleic Acid Res. Mol. Biol.*, **53**, 79–129.
9. Chan,C.T.Y., Dyavauah,M., DeMott,M.S., Taghizadeh,K., Dedon,P.C. and Begley,T.J. (2010) A Quantitative Systems Approach Reveals Dynamic Control of tRNA Modifications during Cellular Stress. *PLoS Genet.*, **6**, e1001247.
10. Begley,U., Dyavaiah,M., Patil,A., Rooney,J.P., DiRenzo,D., Young,C.M., Conklin,D.S., Zitomer,R.S. and Begley,T.J. (2007) Trm9-catalyzed tRNA modifications link translation to the DNA damage response. *Mol. Cell*, **28**, 860–870.
11. Russell,S.P. and Limbach,P.A. (2013) Evaluating the reproducibility of quantifying modified nucleosides from ribonucleic acids by LC–UV–MS. *J. Chromatogr. B*, **923–924**, 74–82.
12. Lui,L. and Lowe,T. (2013) Small nucleolar RNAs and RNA-guided post-transcriptional modification. *Essays Biochem.*, **54**, 53–77.
13. Li,S.C., Tsai,K.W., Pan,H.W., Jeng,Y.M., Ho,M.R. and Li,W.H. (2012) MicroRNA 3′ end nucleotide modification patterns and arm selection preference in liver tissues. *BMC Syst. Biol.*, **6**, S14.
14. Meyer,K.D., Saletore,Y., Zumbo,P., Elemento,O., Mason,C.E. and Jaffrey,S.R. (2012) Comprehensive Analysis of mRNA Methylation Reveals Enrichment in 3′ UTRs and near Stop Codons. *Cell*, **149**, 1635–1646.
15. Carlile,T.M., Rojas-Duran,M.F., Zinshteyn,B., Shin,H., Bartoli,K.M. and Gilbert,W.V. (2014) Pseudouridine profiling reveals regulated mRNA pseudouridylation in yeast and human cells. *Nature*, **515**, 143–146.
16. Linder,B., Grozhik,A.V., Olarerin-George,A.O., Meydan,C., Mason,C.E. and Jaffrey,S.R. (2015) Single-nucleotide-resolution mapping of m6A and m6Am throughout the transcriptome. *Nat. Meth.*, **12**, 767–772.
17. Gaston,K.W. and Limbach,P.A. (2014) The identification and characterization of non-coding and coding RNAs and their modified nucleosides by mass spectrometry. *RNA Biol.*, **11**, 1568–1585.
18. Davis,G.E., Gehrke,C.W., Kuo,K.C. and Agris,P.F. (1979) Major and modified nucleosides in tRNA hydrolysates by high performance liquid chromatography. *J. Chromatogr.*, **173**, 281–298.
19. Gehrke,C.W., Kuo,K.C., McCune,R.A., Gerhardt,K.O. and Agris,P.F. (1982) Quantitative enzymatic hydrolysis of tRNAs: Reversed-phase high-performance liquid chromatography of tRNA nucleosides. *J. Chromatogr. B*, **230**, 297–308.
20. Su,D., Chan,C.T., Gu,C., Lim,K.S., Chionh,Y.H., McBee,M.E., Russell,B.S., Babu,I.R., Begley,T.J. and Dedon,P.C. (2014) Quantitative analysis of ribonucleoside modifications in tRNA by HPLC-coupled mass spectrometry. *Nat. Protoc.*, **9**, 828–841.
21. Rose,R.E., Quinn,R., Sayre,J.L. and Fabris,D. (2015) Profiling ribonucleotide modifications at full- transcriptome level: a step toward MS-based epitranscriptomics. *RNA*, **21**, 1361–1374.
22. Wang,Y., Li,Y., Toth,J.I., Petroski,M.D., Zhang,Z. and Zhao,J.C. (2014) N6-methyladenosine modification destabilizes developmental regulators in embryonic stem cells. *Nat. Cell Biol.*, **16**, 191–198.
23. Chen,T., Hao,Y., Zhang,Y., Li,M., Wang,M., Han,W., Wu,Y., Lv,Y., Hao,J., Wang,L. *et al.* (2015) m6A RNA Methylation Is Regulated by MicroRNAs and Promotes Reprogramming to Pluripotency. *Cell Stem Cell*, **16**, 289–301.
24. Edelheit,S., Schwartz,S., Mumbach,M.R., Wurtzel,O. and Sorek,R. (2013) Transcriptome-Wide Mapping of 5-methylcytidine RNA Modifications in Bacteria, Archaea, and Yeast Reveals m5C within Archaeal mRNAs. *PLoS Genet.*, **9**, e1003602.
25. Cavaluzzi,M.J. and Borer,P.N. (2004) Revised UV extinction coefficients for nucleoside-5′-monophosphates and unpaired DNA and RNA. *Nucleic Acids Res.*, **32**, e13.
26. Brandmayr,C., Wagner,M., Brückl,T., Globisch,D., Pearson,D., Kneuttinger,A.C., Reiter,V., Hienzsch,A., Koch,S., Thoma,I. *et al.* (2012) Isotope-Based Analysis of Modified tRNA Nucleosides Correlates Modification Density with Translational Efficiency. *Angew. Chem. Int. Ed. Engl.*, **51**, 11162–11165.
27. Laourdakis,C.D., Merino,E.F., Neilson,A.P. and Cassera,M.B. (2014) Comprehensive quantitative analysis of purines and pyrimidines in the human malaria parasite using ion-pairing ultra-performance liquid chromatography–mass spectrometry. *J. Chromatogr. B*, **967**, 127–133.
28. Kellner,S., Ochel,A., Thüring,K., Spenkuch,F., Neumann,J., Sharma,S., Entian,K.-D., Schneider,D. and Helm,M. (2014) Absolute and relative quantification of RNA modifications via biosynthetic isotopomers. *Nucleic Acids Res.*, **42**, e142.
29. Shrivastava,A. and Gupta,V. (2011) Methods for the determination of limit of detection and limit of quantitation of the analytical methods. *Chronicles of Young Scientists*, **2**, 21–25.
30. Fasano,C.A., Chambers,S.M., Lee,G., Tomishima,M.J. and Studer,L. (2010) Efficient derivation of functional floor plate tissue from human embryonic stem cells. *Cell Stem Cell*, **6**, 336–347.
31. Van de Leemput,J., Boles,N.C., Kiehl,T.R., Corneo,B., Lederman,P., Menon,V., Lee,C., Martinez,R.A., Levi,B.P., Thompson,C.L. *et al.* (2014) CORTECON: A Temporal Transcriptome Analysis of In Vitro Human Cerebral Cortex Development from Human Embryonic Stem Cells. *Neuron*, **83**, 51–68.
32. Chambers,S.M., Fasano,C.A., Papapetrou,E.P., Tomishima,M., Sadelain,M. and Studer,L. (2009) Highly efficient neural conversion of human ES and iPS cells by dual inhibition of SMAD signaling. *Nat. Biotechnol.*, **27**, 275–280.
33. Gaspard,N., Bouschet,T., Hourez,R., Dimidschstein,J., Naeije,G., van den Ameele,J., Espuny-Camacho,I., Herpoel,A., Passante,L., Schiffmann,S.N. *et al.* (2008) An intrinsic mechanism of corticogenesis from embryonic stem cells. *Nature*, **455**, 351–357.
34. Qian,X., Davis,A.A., Goderie,S.K. and Temple,S. (1997) FGF2 concentration regulates the generation of neurons and glia from multipotent cortical stem cells. *Neuron*, **18**, 81–93.

35. Crain,P.F. (1990) Preparation and enzymatic hydrolysis of DNA and RNA for mass spectrometry. *Meth. Enzymol.*, **193**, 782–790.
36. Luo,G.-Z., MacQueen,A., Zheng,G., Duan,H., Dore,L.C., Lu,Z., Liu,J., Chen,K., Jia,G., Bergelson,J. *et al.* (2014) Unique features of the m6A methylome in Arabidopsis thaliana. *Nat. Commun.*, **5**, 5630.
37. Shih,P., Pedersen,L.G., Gibbs,P.R. and Wolfenden,R. (1998) Hydrophobicities of the nucleic acid bases: distribution coefficients from water to cyclohexane. *J. Mol. Biol.*, **280**, 421–430.
38. Quinn,R., Basanta-Sanchez,M., Rose,R.E. and Fabris,D. (2013) Direct infusion analysis of nucleotide mixtures of very similar or identical elemental composition. *J. Mass Spectrom.*, **48**, 703–712.
39. Dominissini,D., Moshitch-Moshkovitz,S., Salmon-Divon,M., Amariglio,N. and Rechavi,G. (2013) Transcriptome-wide mapping of N6-methyladenosine by m6A-seq based on immunocapturing and massively parallel sequencing. *Nat. Protoc.*, **8**, 176–189.
40. Alarcón,C.R., Lee,H., Goodarzi,H., Halberg,N. and Tavazoie,S.F. (2015) N6-methyladenosine marks primary microRNAs for processing. *Nature*, **519**, 482–485.
41. Squires,J.E., Patel,H.R., Nousch,M., Sibbritt,T., Humphreys,D.T., Parker,B.J., Suter,C.M. and Preiss,T. (2012) Widespread occurrence of 5-methylcytosine in human coding and non-coding RNA. *Nucleic Acids Res.*, **40**, 5023–5033.
42. Cavaillé,J., Buiting,K., Kiefmann,M., Lalande,M., Brannan,C.I., Horsthemke,B., Bachellerie,J.P., Brosius,J. and Hüttenhofer,A. (2000) Identification of brain-specific and imprinted small nucleolar RNA genes exhibiting an unusual genomic organization. *PNAS*, **97**, 14311–14316.
43. Nestler,E.J. (2005) The Neurobiology of Cocaine Addiction. *Sci. Pract. Perspect.*, **3**, 4–10.
44. Martin,C.B.P., Ramond,F., Farrington,D.T., Aguiar,A.S. Jr., Chevarin,C., Berthiau,A.S., Caussanel,S., Lanfumey,L., Herrick-Davis,K., Hamon,M. *et al.* (2013) RNA splicing and editing modulation of 5-HT2C receptor function: relevance to anxiety and aggression in VGV mice. *Mol. Psychiatry*, **18**, 656–665.
45. Agris,P.F. (2008) Bringing order to translation: the contributions of transfer RNA anticodon-domain modifications. *EMBO Rep.*, **9**, 629–635.
46. Blanco,S., Dietmann,S., Flores,J.V., Hussain,S., Kutter,C., Humphreys,P., Lukk,M., Lombard,P., Treps,L., Popis,M. *et al.* (2014) Aberrant methylation of tRNAs links cellular stress to neuro-developmental disorders. *EMBO J.*, **33**, 2020–2039.
47. Li,J.B. and Church,G.M. (2013) Deciphering the functions and regulation of brain-enriched A-to-I RNA editing. *Nat. Neurosci.*, **16**, 1518–1522.
48. Li,S. and Mason,C.E. (2014) The Pivotal Regulatory Landscape of RNA Modifications. *Annu. Rev.Genomics Hum. Genet.*, **15**, 127–150.